
DECISION-MAKING WITH AUTO-ENCODING VARIATIONAL BAYES

A PREPRINT

Romain Lopez^{1,†}, Pierre Boyeau^{1,2}, Nir Yosef^{1,3,4}, Michael I. Jordan^{1,5}, Jeffrey Regier⁶

¹ Department of Electrical Engineering and Computer Sciences,
University of California, Berkeley

² Department of Applied Mathematics and Computer Science,
Ecole des Ponts ParisTech

³ Ragon Institute of MGH, MIT and Harvard, Cambridge

⁴ Chan-Zuckerberg Biohub, San Francisco

⁵ Department of Statistics,
University of California, Berkeley

⁶ Department of Statistics,
University of Michigan, Ann Arbor

[†] Corresponding Author: romain_lopez@berkeley.edu

February 19, 2020

ABSTRACT

To make decisions based on a model fit by Auto-Encoding Variational Bayes (AEVB), practitioners typically use importance sampling to estimate a functional of the posterior distribution. The variational distribution found by AEVB serves as the proposal distribution for importance sampling. However, this proposal distribution may give unreliable (high variance) importance sampling estimates, thus leading to poor decisions. We explore how changing the objective function for learning the variational distribution, while continuing to learn the generative model based on the ELBO, affects the quality of downstream decisions. For a particular model, we characterize the error of importance sampling as a function of posterior variance and show that proposal distributions learned with evidence upper bounds are better. Motivated by these theoretical results, we propose a novel variant of the VAE. In addition to experimenting with MNIST, we present a full-fledged application of the proposed method to single-cell RNA sequencing. In this challenging instance of multiple hypothesis testing, the proposed method surpasses the current state of the art.

Keywords variational inference · variational autoencoders · single-cell transcriptomics · importance sampling · Bayesian statistics

1 Introduction

Variational autoencoders (VAEs) perform model selection by maximizing a lower bound on the model evidence [1, 2]. They find a low-dimensional representation of data that is transformed through a learned nonlinear function (a neural network) to the parameters of a conditional likelihood. VAEs achieve impressive performance on pattern-matching tasks like representation/manifold learning and synthetic image generation [3].

Many machine learning applications, however, require decisions, not just compact representations of the data. Researchers have attempted to use VAEs for decision-making applications too, including novelty detection in control applications [4], mutation-effect prediction from genomic sequences [5], artifact detection [6], and Bayesian hypothesis testing for single-cell RNA sequencing data [7, 8]. To make decisions based on VAEs, these researchers implicitly appeal to Bayesian decision theory, which counsels taking the action that minimizes expected loss under the posterior distribution [9].

However, for VAEs, the relevant functionals of the posterior cannot be computed exactly. Instead, practitioners take one of three approaches. The variational distribution may be used as a surrogate for the posterior [5]. Or, the variational distribution may be used as a proposal distribution for importance sampling. Or, the variational distribution can be ignored after the model is fit, and decisions may be based on an iterative sampling method such as MCMC or annealed importance sampling [10]. But will any of these combined procedures (AEVB for training and one of these methods for approximating posterior expectations) produce good decisions?

They may not, for two reasons. First, estimates of the relevant expectations of the posterior may be biased and/or may have high variance. The former is typical when the variational distribution is substituted for the posterior; the latter is common for importance sampling estimators. By using the variational distribution as a proposal distribution, practitioners aim to get unbiased low-variance estimates of posterior expectations. But this effort often fails. The variational distribution recovered by AEVB, which minimizes the reverse Kullback-Leibler (KL) divergence between the variational distribution and the model posterior, is known to systematically underestimate variance [11, 12], making it arbitrarily bad as an importance sampling proposal distribution. Minimizing either the forward KL divergence or the χ^2 -divergence has more favorable properties for fitting a proposal distribution (Section 2).

Second, even if we can faithfully compute expectations of the model posterior, the model learned by AEVB may not resemble the real data-generating process, for a related reason. AEVB relies on tight lower bounds of the evidence that are based on importance sampling estimates, where the variational distribution is used as a proposal [13]. Therefore, AEVB might not fit the model well.

To address both of these issues, we propose (see Section 3) three new variants of the VAE, which we call Sandwich Bound VAEs (sbVAEs). As in AEVB, we fit the generative model based on an evidence lower bound. However, we use alternating minimization, and choose the variational distribution that minimizes an *upper* bound on the log evidence, equivalent to minimizing either the forward Kullback-Leibler (KL) [14, 15], or the χ^2 divergence [16], instead of the reverse KL divergence. We also consider multiple importance sampling to combine those two proposals.

Our approach is justified theoretically via analysis of concentration bounds of the importance sampling estimators. In Section 4 we exemplify this strategy by providing a complete analysis for the case of probabilistic PCA [17].

We benchmark our variants of the sbVAE against the VAE in three experiments (Section 5). After confirming our theoretical findings empirically for pPCA (Section 5.1), we consider a practical instance of classification-based decision theory problem, and show that underdispersion of the posterior approximation harms performance. sbVAEs outperforms all alternatives in this case (Section 5.2). We then present a scientific case study, focusing on an instance of multiple hypothesis testing in single-cell RNA sequencing data, where show that our approach yields a better calibrated estimate of the expected posterior False Discovery Rate (FDR) when compared to the current state-of-the-art approach (Section 5.3).

2 Background

Bayesian decision making [9] makes use of a model and its posterior distribution to make optimal decisions. We bring together several lines of research in an overall Bayesian framework.

2.1 Auto-encoding variational Bayes

Variational Autoencoders [1] are based on a hierarchical Bayesian model [18]. Let x be the observed random variables and z the latent variables. To learn a generative model $p_\theta(x, z)$ that maximizes the evidence $\log p_\theta(x)$, variational Bayes [11] uses a proposal distribution $q_\phi(z | x)$ to approximate the posterior $p_\theta(z | x)$. The evidence decomposes as

the *evidence lower bound* (ELBO) and the reverse KL variational gap (VG):

$$\underbrace{\log p_\theta(x)}_{\text{evidence}} = \underbrace{\mathbb{E}_{q_\phi(z|x)} \log \frac{p_\theta(x, z)}{q_\phi(z|x)}}_{\text{ELBO}} + \underbrace{\Delta_{\text{KL}}(q_\phi \| p_\theta)}_{\text{reverse KL VG}}. \quad (1)$$

Here we adopted the condensed notation $\Delta_{\text{KL}}(q_\phi \| p_\theta)$ to refer to the KL divergence between $q_\phi(z|x)$ and $p_\theta(z|x)$. In the light of this decomposition, a valid inference procedure is to jointly maximize the ELBO with respect to the model's parameters as well as the variational distribution. The resulting variational distribution minimizes the reverse KL divergence. VAEs parameterize the variational distribution with a neural network. Stochastic gradients of the ELBO with respect to the variational parameters are computed via the reparameterization trick [1].

2.2 Evidence upper bounds for approximate inference

Although variational inference traditionally maximizes a lower bound on the marginal likelihood, upper bounds on the marginal likelihood can be minimized instead. [15] decompose the evidence into the *evidence upper bound* (EUBO) and the forward KL VG:

$$\underbrace{\log p_\theta(x)}_{\text{evidence}} = \underbrace{\log \mathbb{E}_{p_\theta(z|x)} \frac{p_\theta(x, z)}{q_\phi(z|x)}}_{\text{EUBO}} - \underbrace{\Delta_{\text{KL}}(p_\theta \| q_\phi)}_{\text{forward KL VG}}. \quad (2)$$

[16] decompose the evidence using a χ^2 divergence:

$$\underbrace{\log p_\theta(x)}_{\text{evidence}} = \underbrace{\frac{1}{2} \log \mathbb{E}_{q_\phi(z|x)} \left(\frac{p_\theta(x, z)}{q_\phi(z|x)} \right)^2}_{\text{CUBO}} - \underbrace{\frac{1}{2} \log (1 + \Delta_{\chi^2}(p_\theta \| q_\phi))}_{\chi^2 \text{ VG}}. \quad (3)$$

The choice of ELBO, EUBO, and CUBO matters most when the posterior does not belong to the variational family, as is typically the case. The properties of the variational distribution (mode-seeking or mass-covering) depends highly on the geometry of the variational gap [19].

2.3 Approximation of posterior expectations

Given a model p_θ , an action set \mathcal{A} , and a loss L , the optimal decision $a^*(x)$ for observation x is an expectation taken with respect to the posterior:

$$\mathcal{Q}(f, x) = \mathbb{E}_{p_\theta(z|x)} f(z). \quad (4)$$

Here f depends on the loss [9]. We therefore focus on numerical methods for estimating $\mathcal{Q}(f, x)$. Evaluating these expectations is the aim of Markov chain Monte Carlo, annealed importance sampling (AIS) [20], and variational methods [21].

Although we typically do not have direct access to the posterior $p_\theta(z|x)$, we can, however, sample $(z_i)_{1 \leq i \leq n}$ from the variational distribution $q_\phi(z|x)$. A naive, but practical, approach is to consider a plugin estimator [4, 5, 6, 7]:

$$\hat{\mathcal{Q}}_{\text{P}}^n(f, x) = \frac{1}{n} \sum_{i=1}^n f(z_i), \quad (5)$$

which replaces the exact posterior by sampling z_1, \dots, z_n from $q_\phi(z|x)$. A less naive approach is to use importance sampling (IS):

$$\hat{\mathcal{Q}}_{\text{IS}}^n(f, x) = \frac{1}{n} \sum_{i=1}^n w(x, z_i) f(z_i), \quad (6)$$

with importance weights

$$w(x, z) := \frac{p_\theta(z|x)}{q_\phi(z|x)}. \quad (7)$$

The nonasymptotic behavior of both estimators is well understood. In particular, we have the following error bounds.

Proposition 1. (Deviation for posterior expectation estimates) *Let \mathcal{F} be a set of test functions uniformly bounded by 1 on \mathcal{Z} . Let $f \in \mathcal{F}$ and $\eta \in \mathbb{R}_+^*$. With probability at least $1 - \eta$ in (z_1, \dots, z_n) , we have that*

$$\begin{aligned} |\hat{Q}_P^n(f, x) - \mathcal{Q}(f, x)| &\leq \sqrt{\frac{\ln 1/\eta}{2n}} + \sqrt{\Delta_{\text{KL}}(p_\theta \parallel q_\phi)} \\ |\hat{Q}_{\text{IS}}^n(f, x) - \mathcal{Q}(f, x)| &\leq \frac{2B \ln 1/\eta}{3n} + \sqrt{\frac{2\Delta_{\chi^2}(p_\theta \parallel q_\phi) \ln 1/\eta}{n}}, \end{aligned}$$

where $B = \sup_{z \in \mathcal{Z}} w(x, z)$.

The proof for IS appears in Theorem 1 of [22], and we have constructed a similar proof for the plugin estimator using Hoeffding’s Lemma and Pinsker’s Inequality; see Appendix A. Two important quantities appear in the error bounds of Proposition 1 for inexact variational approximations: the plugin estimator bias is bounded by the forward KL divergence while the IS estimator variance is bounded by the χ^2 divergence.

The numerous variants of IS used in practice such as the weight normalization or thresholding [23], have similar theoretical properties; their error is bounded as a function of the χ^2 divergence (see Theorem 2.1 in [24]). Controlling the χ^2 divergence also controls the forward KL divergence:

$$\exp\{\Delta_{\text{KL}}(p_\theta \parallel q_\phi)\} \leq \Delta_{\chi^2}(p_\theta \parallel q_\phi). \quad (8)$$

However, bounding the reverse KL divergence $\Delta_{\text{KL}}(q_\phi \parallel p_\theta)$, as is done with AEVB, gives no assurance of the quality of the posterior as a proposal distribution. Furthermore, in all cases where variational inference does not yield the exact posterior, the reverse KL is known to underestimate the variance of the posterior density [12], which can produce arbitrarily bad proposal distributions for estimation of posterior expectations.

More recently, [25] showed that the χ^2 divergence may not characterize the sample size needed in IS. For a fixed x , their concentration bound implies that if the random variable $\log w(x, z)$ concentrates around its mean under the posterior $p_\theta(z \mid x)$, then $\exp\{\Delta_{\text{KL}}(p_\theta \parallel q_\phi)\}$ is a sufficient and necessary number of samples for estimating the posterior expectation $\mathcal{Q}(f, x)$. It is not currently understood whether this concentration hypothesis holds for arbitrary VAEs.

3 Sandwich Bounds for VAEs

Based on Proposition 1, we introduce new training and decision-making methods for VAEs that use sandwich bounds and alternating optimization (Algorithm 1). To update the generative model p_θ at each step of an iterative optimization procedure, we use the gradients of the importance weighted ELBO (IWELBO) [13, 21] with a fixed proposal $q_\phi(z \mid x)$. To update the proposal distribution $q_\phi(z \mid x)$, with p_θ fixed, we minimize the right-hand side of Proposition 1. Because neither of these quantities are available in closed form, we use known upper bounds on the evidence. Minimizing EUBO in Equation (2) at fixed p_θ is equivalent to minimizing the forward KL divergence. Similarly, minimizing CUBO in Equation (3) at fixed p_θ is equivalent to minimizing the χ^2 divergence. We compute stochastic estimates of the gradients of the objective using importance sampling (IS). We also consider mixtures of the two variational distribution for multiple IS.

This alternate minimization scheme is similar in spirit to the reweighted wake-sleep algorithm [26, 14], although without the sleep phase, and with a more general class of objectives for updating the proposal. Because our framework makes use of both an upper bound and a lower bound of the evidence for inference, we refer to it as learning VAEs with Sandwich Bounds (sbVAEs). The first sbVAE variant, which we refer to as the KL-sbVAE, consists in using EUBO as an upper bound and is equivalent to the reweighted wake sleep algorithm without a sleep-phase (Wake-Wake) [27]. Our framework generalizes the Wake-Wake algorithm for arbitrary upper bounds on the model evidence. For example, the second sbVAE variant (χ -sbVAE) uses instead CUBO as an upper bound of the evidence.

Selecting the best upper bound is a hard problem as it depends on the generative model, the shape of the candidate variational distributions, its amortization scheme and possibly the decision loss. As a more systematic solution, we propose a third variant of sbVAE, which we call M-sbVAE, that uses multiple importance sampling [28] in order to combine variational distributions from the KL-sbVAE and the χ -sbVAE. For $\beta \in (0, 1)$, we create a mixture distribution \bar{q} defined as

$$\bar{q} = (1 - \beta)q_{\text{EUBO}} + \beta q_{\text{CUBO}}. \quad (9)$$

In the M-sbVAE, \bar{q} is used as a proposal to learn a generative model as well as for estimating posterior expectations, using only the partial updates for θ in Algorithm 1.

After convergence of the model’s and the variational distribution’s parameters, we perform decisions using importance sampling with $q(z \mid x)$ (or \bar{q}) as a proposal.

Algorithm 1 KL-sbVAE and χ -sbVAE**Require:** $\alpha \leftarrow 1$ for KL-sbVAE and 2 for χ -sbVAE

- 1: $\theta, \phi \leftarrow$ Initialize parameters
 - 2: **repeat**
 - 3: $X^M \leftarrow$ Random minibatch of M observations from the training set
 - 4: $Z^{M,K} \leftarrow K$ samples from the variational posterior $q(z | x_i)$ for each observation x_i .
 - 5: $W^{M,K} \leftarrow$ unnormalized importance weights w
 - 6: $g_\theta = \frac{1}{M} \sum_{m=1}^M \sum_{k=1}^K \frac{w_{m,k}}{\sum_{k'} w_{m,k'}} \nabla_\theta \log p_\theta(x_m, z_{m,k})$
 - 7: $g_\phi = \frac{1}{M} \sum_{m=1}^M \sum_{k=1}^K \frac{w_{m,k}^\alpha}{\sum_{k'} w_{m,k'}^\alpha} \nabla_\phi \log q_\phi(z_{m,k} | x_m)$
 - 8: $\theta, \phi \leftarrow$ Update parameters using gradients g_θ, g_ϕ
 - 9: **until** convergence of parameters (θ, ϕ)
- output** θ, ϕ

4 Theoretical Analysis for pPCA

We aim to understand theoretically the advantages and disadvantages of these various decision-making procedures. Because intractability prevents us from deriving sharp constants for arbitrary models, here we consider probabilistic principal component analysis (pPCA) [29]. pPCA is a linear model for which posterior inference is tractable. Though the analysis is a special case, we believe that it gives intuition for performance of our decision-making procedures more generally because, for many models used in practice, a Gaussian distribution approximates the posterior well, as demonstrated by the success of the Laplace approximation [30].

In pPCA, the latent variables z generate data x . We use an isotropic Gaussian prior on z and a linear model with spherical Gaussian observation model for x :

$$\begin{aligned} p_\theta(z) &= \text{Normal}(0, I) \\ p_\theta(x | z) &= \text{Normal}(Wz + \mu, \sigma^2 I). \end{aligned} \quad (10)$$

In this setting, $\theta := (W, \mu, \sigma)$. We consider an amortized posterior approximation

$$q_\phi(z | x) = \text{Normal}(h_\eta(x), D(x)), \quad (11)$$

where $D(x)$ is a diagonal covariance matrix $\text{diag}(h_\xi(x))$. h_η (resp. h_ξ) is a neural network with parameters η (resp. ξ). In this example, $\phi = (\eta, \xi)$.

From the invariance properties of Gaussian distributions [31], our next lemma gives concentration bounds for the log-ratio statistics under the posterior.

Lemma 1. (Concentration of the log-likelihood ratio) *For an observation x , let Σ be the variance of the posterior distribution under the pPCA model, $p_\theta(z | x)$. Let*

$$A(x) = \Sigma^{1/2} [D(x)]^{-1} \Sigma^{1/2} - I. \quad (12)$$

For z following the posterior distribution, $\log w(x, z)$ is a sub-exponential random variable. Further, there exists a $t^(x)$ such that, under the posterior $p_\theta(z | x)$ and for all $t > t^*(x)$,*

$$\mathbb{P}(|\log w(x, z) - \Delta_{\text{KL}}(p_\theta \| q_\phi)| \geq t) \leq e^{-\frac{t}{8\|A(x)\|_2}}, \quad (13)$$

This lemma characterizes the concentration of the log-likelihood ratio, a central quantity to all the VAE variants we introduce, as the spectral norm of a simple matrix $\|A(x)\|_2$. Plugging in the concentration bound from Lemma 1 in the result of in [25], we obtain an error bound on the IS estimator for posterior expectations.

Theorem 1. (Sufficient sample size) *For an observation x , suppose that the second moment of $f(z)$ under the posterior is bounded by κ . If the number of particles for importance sampling n satisfies $n = \exp\{\Delta_{\text{KL}}(p_\theta \| q_\phi) + t\}$ for some $t > t^*(x)$, then*

$$\mathbb{E}|\hat{\mathcal{Q}}_{\text{IS}}^n(f, x) - \mathcal{Q}(f, x)| \leq 3\sqrt{\kappa}e^{-t/4\gamma}, \quad (14)$$

with $\gamma = \max(1, 4\|A(x)\|_2)$

Theorem 1 identifies a key quantity—the spectral norm of $A(x)$ —as useful for controlling the error of the IS estimator. As $\|A(x)\|_2$ is smaller for larger values of $D(x)$, we recover the known fact that overestimating variance is always better than underestimating variance for IS.

As a consequence of this result, we can characterize the behavior of several algorithms, in particular those based on minimizing ELBO, EUBO, and CUBO. We provide this analysis for a bivariate Gaussian example, in which all the quantities of interest can be visualized (full derivations in Appendix B). Figure 1 shows that the ELBO underestimates the variance while both upper bounds provide good coverage of the posterior. $\|A\|_2$ is significantly smaller for EUBO and CUBO compared to for the ELBO.

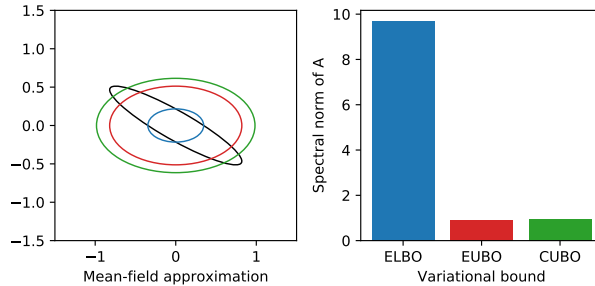


Figure 1: Mean-field approximation to the inference for the bivariate pPCA example using several variational bounds and corresponding values of $\|A\|_2$.

Taken together, these results suggest that learning the parameters of the variational distribution based on upper-bound minimization provides a better proposal for importance sampling compared to the ELBO. This proposal can be used in learning a better generative model as well as better assessment of posterior expectations.

Analysis of Gaussian VAEs If we replace the linear function in Equation (10) with a neural network with rectified linear unit activations, the posterior is sub-Gaussian (Our proof appears in Appendix C.) Under this setting, we can further prove a sub-exponential upper-tail bound for the log-likelihood ratio, which ensures that the main concentration hypothesis of [25] holds. However, the intractability does not allow us to characterize the optimal sub-exponential rate, unlike the pPCA example. Further work might focus on deriving sharp bounds in the one-layer VAE case.

5 Experiments

We explore three experimental settings. First, we consider synthetic data drawn from probabilistic principal component analysis (pPCA), as this setting most directly illustrates the consequences of Theorem 1. Second, we consider MNIST digit classification [32] with a “reject” option. Third, we detect differentially expressed genes in single-cell RNA sequencing data (scRNA-seq).

To evaluate the learned generative model, we provide goodness of fit metrics based on IWELBO and CUBO on held-out data, which are proxies for the log-likelihood. Also, we report the Pareto-smoothed importance sampling (PSIS) diagnostic \hat{k} for diagnosis of variational inference [23]. PSIS is computed by fitting a generalized Pareto distribution to the IS weights; it indicates the viability of the variational distribution for IS. We report the median PSIS over 64 observations, using 10,000 samples from the posterior.

When not stated otherwise, we use Adam [33] for optimization of θ and ϕ . We use 25 importance samples per iteration for training the models, 10,000 samples for reporting log-likelihood proxies and 200 samples for making decisions. We ran our experiments on a machine with a single NVIDIA GeForce RTX 2070 GPU.

5.1 Probabilistic PCA

To build intuition, we assess how well different variants of VAEs can estimate posterior expectations under the pPCA model described in Eq. (10). We use a linear function for the mean and for the log-variance of the variational distribution. This is a popular setup for approximate inference diagnostics [12] since the posterior has an analytic form, and the form is not typically mean-field. We generate synthetic data according to the pPCA model and compute the posterior $p_\theta(z | x)$. Let e_1 be the first vector of the canonical basis of \mathbb{R}^d . To show robustness, we retain a family $(f_\nu)_{\nu>0}$ of step functions defined as $f_\nu(z) = \mathbb{1}\{e_1^\top z \geq \nu\}$ for $\nu > 0$ and $z \in \mathcal{Z}$. The resulting posterior expectation is tractable

Table 1: Results on the pPCA simulated data. The standard errors are derived from 10 random initializations for each method. The marginal log likelihood (higher is better) is between IWELBO and CUBO.

	VAE	KL-sbVAE	χ -sbVAE	M-sbVAE
IWELBO	-17.42 \pm 0.05	-16.96 \pm 0.03	-16.94 \pm 0.02	-16.94 \pm 0.01
CUBO	-16.36 \pm 0.07	-16.08 \pm 0.02	-15.96 \pm 0.03	-16.04 \pm 0.03
PSIS	0.68 \pm 0.02	0.43 \pm 0.02	0.36 \pm 0.02	0.36 \pm 0.01
$\ A\ _2$	7.699 \pm 5.496	1.744 \pm 0.673	1.085 \pm 0.293	-

since it can be written as $\mathcal{Q}(f, x) = p_\theta(z_1 \geq \nu | x)$, which is the cumulative density function of a Gaussian distribution. Appendix D contains further details for this experiment.

Table 1 contains our results. All sbVAEs learn a better generative model and outperform the original VAE both in terms of upper bounds on the evidence (CUBO) and lower bound of the evidence (IWELBO).

Although all algorithms yield a reasonable value for the PSIS diagnostic, χ -sbVAE’s value is significantly better. This is anticipated by our theory because the latter has a small spectral norm of A . Figure 2 shows that the sbVAEs works better than the original VAE at estimating posterior expectations.

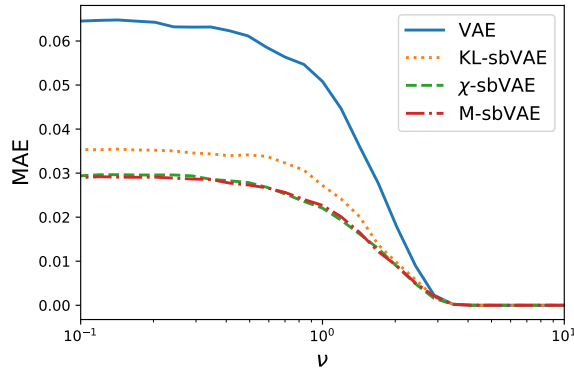


Figure 2: Mean absolute error of posterior expectation estimation for different values of ν .

5.2 Classification-based decision theory

We consider the MNIST dataset [32], which includes features x for each the image of handwritten digits and a label c . We aim to predict whether or not x has its label included in a given subset of labels (the digits one through eight). We also allow no decision to be made for ambiguous cases (the “reject” option) [17]. As a generative model, we use the M1+M2 model for semi-supervised learning [34].

We split the MNIST dataset [32] evenly between training and test datasets. For the labels from 0 to 8, we use 1,500 labeled examples in total. All the images associated with label 9 are unlabelled. We assume in this experiment that the MNIST dataset has $C = 9$ classes (i.e., $c \in \{1, \dots, C\}$) and that we have a posterior probability for the class $p_\theta(c | x)$, for a model yet to be defined. Let $L(a, c)$ be the loss defined over the action set $\mathcal{A} = \{\emptyset, 1, \dots, C\}$. Action \emptyset is known as the rejection option in classification (we wish to reject the label 9 at decision time). For this loss, it is known that the optimal decision $a^*(x)$ is a threshold-based rule [17] on the posterior probability. This is a fundamentally different configuration than classical classification because making an informed decision requires knowledge of the full posterior $p_\theta(c | x)$ and not only the maximum probability class. This rule can be written as a posterior expectation $\mathcal{Q}(f, x)$ for $z = c$ and f a constant unit function. To our knowledge, this is the first time semi-supervised generative models have been evaluated for such a decision-making scenario.

In the M1+M2 model, discrete latent variable c represents the class. Latent variable u is a low-dimensional vector encoding additional variation (not contained in c). Latent variable z is a low-dimensional representation of the observation, drawn from a mixture distribution with mixture assignment c and mixture parameters that are a function of u . The generative model is

$$p_\theta(x, z, c, u) = p_\theta(x | z)p_\theta(z | c, u)p_\theta(c)p_\theta(u). \tag{15}$$

Table 2: Results for the M1+M2 model on MNIST. The standard errors are derived from five random initializations for each method. The marginal log likelihood (higher is better) is between IWELBO and CUBO. AUPRC refers to the area under of the PR curve for rejecting the label 9.

	VAE	KL-SBVAE	χ -SBVAE	M-SBVAE
IWELBO	-110.51 \pm 0.28	-111.96 \pm 0.63	-114.60 \pm 0.41	-101.73 \pm 1.99
CUBO	-103.55 \pm 0.22	-108.66 \pm 0.65	-100.63 \pm 0.57	-95.72 \pm 2.06
AUPRC	0.18 \pm 0.02	0.40 \pm 0.04	0.23 \pm 0.01	0.30 \pm 0.03
PSIS	1.08 \pm 0.03	1.04 \pm 0.04	1.11 \pm 0.01	1.10 \pm 0.03

The variational distribution factorizes as

$$q_\phi(z, c, u | x) = q_\phi(z | x)q_\phi(c | z)q_\phi(u | z, c). \tag{16}$$

Because the reverse KL divergence can cover only one mode of the distribution, it is more prone to attributing zero probabilities to many classes while alternate divergences would penalize that behavior. Appendix E makes this point clear and emphasizes why the M1+M2 model trained as a VAE may reach overconfidence in its posterior.

sbVAEs have the potential to remedy these problems. We derive updates for learning sbVAEs for the M1+M2 model (Appendix F) by marginalizing over latent variable c for unlabelled observations. We consider the problem of deriving estimates from samples in the setting of high number of labels [35] as future work. We learn a M1+M2 model with only nine classes and consider as ground truth that images with label 9 should be rejected at decision time. We used the same architecture for the parameterization of the model and the same amortization as in [34].

Table 2 gives our results, which vary greatly for AUPRC for rejection of label 9 (non attributed) as well as for goodness of fit metrics. We also report PR-ROC curves for the rejection option in Figure 3, in which we see that all sbVAEs greatly outperform the VAE, with a preference for the KL-sbVAE and the M-sbVAE. sbVAEs based on a unique proposal distribution do not seem to provide a better model than the VAE. However, the M-sbVAE does outperform the VAE in terms of IWELBO and CUBO. The accuracy of the classifier on the other labels is similar between all methods (between 92% and 93%). Remarkably, the PSIS diagnosis estimates are greater than one for all algorithms. This indicates that the variational distribution may lead to large estimation error if used as a proposal. This is expected as there are many latent variables in this model with some discrete and other continuous. Still, these results suggest that sbVAEs better quantify uncertainties, even with a high PSIS value.

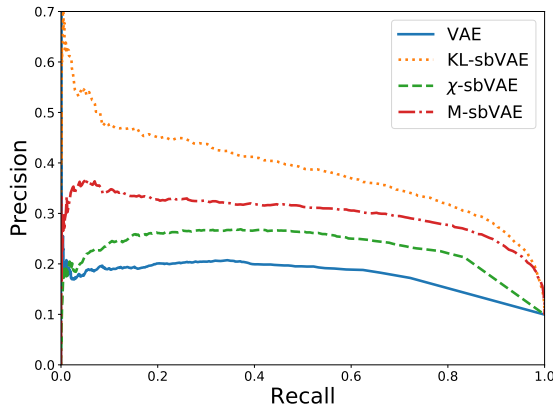


Figure 3: Precision-recall curves for rejecting the label 9 on the MNIST dataset.

5.3 Multiple hypothesis testing

We present an experiment involving Bayesian hypothesis testing in the domain of differentially expressed genes from single-cell transcriptomics data, a central problem in modern molecular biology. Single-cell RNA sequencing data (scRNA-seq) gives a noisy snapshot of the gene expression levels of cells [36, 37]. It can reveal cell types, as well as

Table 3: Results for the scVI model. The standard errors are based on five random initializations for each method (except AIS, only run once). The marginal log likelihood (higher is better) is between IWELBO and CUBO. †: same as VAE. ‡: same as M-sbVAE.

	VAE	VAE + AIS	KL-sbVAE	χ -sbVAE	M-sbVAE + AIS	M-sbVAE
IWELBO	-3329.27 \pm 0.51	†	-3327.05 \pm 0.60	-3325.45 \pm 0.23	‡	-3322.51 \pm 0.19
CUBO	-3327.56 \pm 0.46	†	-3325.46 \pm 0.64	-3323.89 \pm 0.22	‡	-3321.56 \pm 0.17
$\bar{\mu}$ FDR	0.14 \pm 0.01	0.13	0.12 \pm 0.01	0.10 \pm 0.01	0.10	0.10 \pm 0.01
$\bar{\mu}$ TPR	0.40 \pm 0.01	0.42	0.40 \pm 0.01	0.42 \pm 0.01	0.41	0.42 \pm 0.01
PSIS	0.80 \pm 0.09	0.72	0.52 \pm 0.07	0.64 \pm 0.05	0.61	0.33 \pm 0.07

gene markers for each cell type, as long as we have an accurate noise model [38]. scRNA-seq data is a cell-by-gene matrix X , with entry X_{ng} for cell n and gene g . Here we take as given that each sample is mapped to a cell type label c_n .

Single-cell Variational Inference (scVI, [7], Appendix G further details the generative model) models scRNA-seq data with a latent variables h_{ng} representing the underlying gene expression level for gene g in cell n , corrected for a certain number of technical variations (e.g., sequencing depth effects). These underlying expression levels are more reflective of the real proportion of gene expression than the raw data X [39]. Log-fold changes based on h_{ng} can be used to detect differential expression (DE) of gene g across cell types a and b [40, 41]. Indeed, Bayesian decision theory helps decide between a model of the world \mathcal{M}_1^g in which gene g is DE and an alternative model \mathcal{M}_0^g of non-DE.

$$\mathcal{M}_1^g : \left| \log \frac{h_{ag}}{h_{bg}} \right| \geq \delta \quad \text{and} \quad \mathcal{M}_0^g : \left| \log \frac{h_{ag}}{h_{bg}} \right| < \delta, \quad (17)$$

where δ is a threshold defined by the practitioner. DE can therefore be performed by posterior estimation of log-fold change between two cells x_a, x_b , which can be written as

$$p_\theta \left(\left| \log \frac{h_{ag}}{h_{bg}} \right| \geq \delta \mid x_a, x_b \right), \quad (18)$$

and estimated with importance sampling. The optimal decision rule for 0-1 loss is a threshold based on the posterior log-fold change estimate. Rather than directly setting this threshold, we directly control the false discovery rate (FDR) to some level $f_0 \in (0, 1)$.

Let d_g be the (unknown) binary random variable denoting whether gene g is DE. Consider the multiple binary decision rule $\mu^k = (\mu_g^k, g \in G)$ that consists in tagging DE the k genes with the highest posterior estimate of log-fold change. With this notation, the traditional FDR of such a decision rule is

$$\text{FDR} = \mathbb{E} \left[\frac{\sum_g (1 - d^g) \mu_g^k}{\sum_g \mu_g^k} \right]. \quad (19)$$

Following [42], we define the posterior expected FDR as

$$\overline{\text{FDR}} := \mathbb{E} \left[\frac{\sum_g (1 - d^g) \mu_g^k}{\sum_g \mu_g^k} \mid x_a, x_b \right], \quad (20)$$

which can be computed from the differential expression probabilities of Equation (18).

We then set k so that it is the maximum value for which the posterior expected FDR is below f_0 . In this case, estimating the quantity in Equation (20) is equivalent to estimating as many posterior expectations as the total number of genes. We denote by $\bar{\mu}$ the decision rule associated with the threshold 0.10.

We fit the scVI model with the standard VAE procedure as well as all three sbVAE algorithms. We add two baselines based on annealed importance sampling (AIS) [20]. AIS is used to approximate the posterior distribution once the model is fitted. This includes the VAE + AIS and the M-sbVAE + AIS baselines. AIS is computationally intensive, so we used 500 steps and 100 samples from the prior to keep a reasonable runtime. Because the ground-truth FDR cannot be computed on real data, we generated scRNA-seq data using SymSim [43]. SymSim is a simulator that draws measurements from a Beta-Poisson marginal distribution for each cell and gene and adds technical noise by downsampling to reflect both biological signal and technicalities of the experimental protocol. We generated count data from five distinct cells types corresponding to 10,000 cells and 1,000 genes.

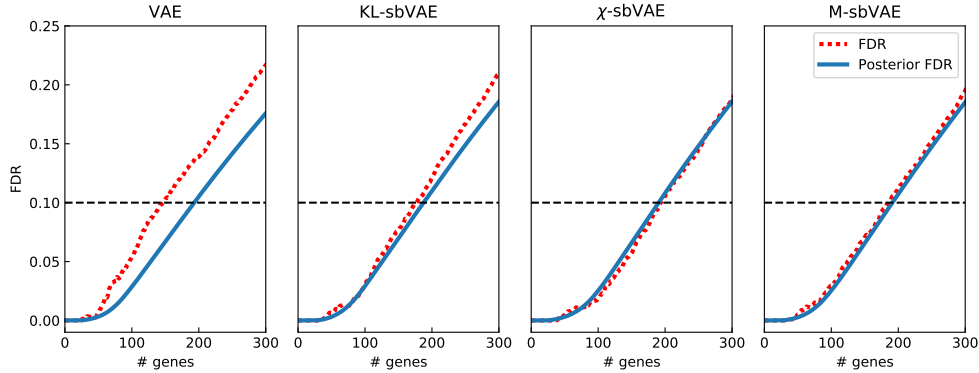


Figure 4: Posterior expected FDR (blue) and ground-truth FDR (red) of the decision rules consisting in selecting the genes with the highest DE probability for the different models.

All three sbVAEs provide a better fit to the data in terms of IWELBO and CUBO, and M-sbVAE performs best (Table 3). Posterior uncertainty plays an essential role in differential expression estimation, especially when conditioning on a small number of cells. As shown in Table 3, $\bar{\mu}$ posterior expected FDR of sbVAEs are properly calibrated, whereas VAE’s detects too many genes. Figure 4 further highlights this point, and shows that M-sbVAE and χ -sbVAE best matches the FDR target curve. We notice that running AIS after inference is much more computationally intensive (14.5 times longer per posterior evaluation). VAE + AIS yields a better proposal than the VAE itself both in terms of PSIS diagnostic and multiple hypothesis testing. We also notice that the M-sbVAE + AIS yields an on-target FDR, which shows that using the mixture \bar{q} we might have learned a better model. Still the proposal distribution from M-sbVAE + AIS does not substantially improve over \bar{q} from the M-sbVAE, especially in terms of PSIS diagnosis. Taken together, these results suggests that the M-sbVAE provides an extremely competitive model fit as well as a framework for decision-making.

6 Discussion

We have proposed three sbVAEs—novel variants of the variational autoencoder—based on alternate minimization between ELBO and upper bounds such as EUBO or CUBO. The analytically derived error of the IS estimator suggests that upper bounds minimization yields a more suitable proposal distribution compared to ELBO for the pPCA model. Our numerical experiments show that in important real-world examples the sbVAE outperforms the VAE but also the VAE followed by AIS. sbVAEs are therefore especially suitable for Bayesian decision-making.

[16] discusses of the numerical stability of the exponentiated CUBO. More recently, [44] found that CUBO might be sensitive to initialization and require an impractical number of samples. We did not encounter such instabilities in our experiments, possibly due to the regularization that comes from amortized inference.

An alternative approach to decision-making is the elegant framework of loss-calibrated inference [45, 46], which further adapts the ELBO to take into account the loss function L . Loss-calibrated inference is not directly applicable because adapting the ELBO for a specific decision-making loss implies a significant bias in learning p_θ . Still, developing hybrid algorithms could be a direction for future research.

Our procedure makes use of both of the forward KL divergence and the χ^2 divergence because of their role in upper bounding the error of the IS estimator. However, the suitability of a given divergence for variational inference depends on the generative model as well as the choice of the variational family. Better performance perhaps could be achieved with a family of divergences that interpolates between forward KL and χ^2 , such as the R enyi divergence family [47]. Tail adaptive algorithms [48] might help to select the best performing R enyi divergence.

Code availability

Code for reproducing the experiments of the paper is available at <https://github.com/PierreBoyeau/sbVAE>.

Acknowledgments

We thank Chenling Xu for useful conversations that helped frame the second experiment. We thank Adam Kosiosek and Tuan-Anh Le for answering questions about implementation details of the Wake-Wake algorithm. NY and RL were supported by grant U19 AI090023 from NIH-NIAID.

References

- [1] Diederik P Kingma and Max Welling. Auto-encoding variational Bayes. In *International Conference on Learning Representations*, 2014.
- [2] Danilo Jimenez Rezende, Shakir Mohamed, and Daan Wierstra. Stochastic backpropagation and approximate inference in deep generative models. In *International Conference on Machine Learning*, 2014.
- [3] Ishaan Gulrajani, Kundan Kumar, Faruk Ahmed, Adrien Ali Taiga, Francesco Visin, David Vazquez, and Aaron Courville. PixelVAE: a latent variable model for natural images. In *International Conference on Learning Representations*, 2017.
- [4] Alexander Amini, Brandon Araki, Daniela Rus, Wilko Schwarting, Guy Rosman, Sertac Karaman, and Daniela L Rus. Variational autoencoder for end-to-end control of autonomous driving with novelty detection and training de-biasing. In *International Conference on Intelligent Robots and Systems*, 2018.
- [5] Adam J. Riesselman, John B. Ingraham, and Debora S. Marks. Deep generative models of genetic variation capture the effects of mutations. *Nature Methods*, 2018.
- [6] Jiarui Ding, Anne Condon, and Sohrab P Shah. Interpretable dimensionality reduction of single cell transcriptome data with deep generative models. *Nature communications*, 2018.
- [7] Romain Lopez, Jeffrey Regier, Michael B. Cole, Michael I. Jordan, and Nir Yosef. Deep generative modeling for single-cell transcriptomics. *Nature Methods*, 2018.
- [8] Chenling Xu, Romain Lopez, Edouard Mehlman, Jeffrey Regier, Michael I. Jordan, and Nir Yosef. Harmonization and annotation of single-cell transcriptomics data with deep generative models. *bioRxiv*, 2019.
- [9] James Berger. *Statistical Decision Theory and Bayesian Analysis*. Springer Science, 1985.
- [10] Yuhuai Wu, Yuri Burda, Ruslan Salakhutdinov, and Roger Grosse. On the quantitative analysis of decoder-based generative models. In *International Conference on Learning Representations*, 2017.
- [11] Martin J Wainwright and Michael I Jordan. Graphical models, exponential families, and variational inference. *Foundations and Trends in Machine Learning*, 2008.
- [12] Richard Eric Turner and Maneesh Sahani. Two problems with variational expectation maximisation for time-series models. Technical report, Gatsby Computational Neuroscience Unit, 2011.
- [13] Yuri Burda, Roger B. Grosse, and Ruslan Salakhutdinov. Importance weighted autoencoders. In *International Conference on Learning Representations*, 2016.
- [14] Jörg Bornschein and Yoshua Bengio. Reweighted wake-sleep. In *International Conference on Learning Representations*, 2015.
- [15] Chunlin Ji and Haige Shen. Stochastic variational inference via upper bound. In *NeurIPS workshop on Bayesian Deep Learning*, 2019.
- [16] Adji Bousso Dieng, Dustin Tran, Rajesh Ranganath, John Paisley, and David Blei. Variational inference via chi-square upper bound minimization. In *Advances in Neural Information Processing Systems*, 2017.
- [17] Christopher M. Bishop. *Pattern Recognition and Machine Learning*. Springer-Verlag, 2006.
- [18] Andrew Gelman and Jennifer Hill. *Data Analysis Using Regression and Multilevel/Hierarchical Models*. Cambridge University Press, 2007.
- [19] Futoshi Futami, Issei Sato, and Masashi Sugiyama. Variational inference based on robust divergences. In *International Conference on Artificial Intelligence and Statistics*, 2018.
- [20] Radford M Neal. Annealed importance sampling. *Statistics and computing*, 2001.
- [21] Justin Domke and Daniel R Sheldon. Importance weighting and variational inference. In *Advances in Neural Information Processing Systems*, 2018.
- [22] Corinna Cortes, Yishay Mansour, and Mehryar Mohri. Learning bounds for importance weighting. In *Advances in Neural Information Processing Systems*, 2010.
- [23] Yuling Yao, Aki Vehtari, Daniel Simpson, and Andrew Gelman. Yes, but did it work?: Evaluating variational inference. In *International Conference on Machine Learning*, 2018.
- [24] S Agapiou, O Papaspiliopoulos, D Sanz-Alonso, and A M Stuart. Importance sampling: Intrinsic dimension and computational cost. *Statistical Science*, 2017.
- [25] Sourav Chatterjee and Persi Diaconis. The sample size required in importance sampling. *The Annals of Applied Probability*, 2018.

- [26] Geoffrey E. Hinton, Peter Dayan, Brendan J. Frey, and Radford M. Neal. The “wake-sleep” algorithm for unsupervised neural networks. *Science*, 1995.
- [27] Tuan Anh Le, A Kosiorek, N Siddharth, Yee Whye Teh, and Frank Wood. Revisiting reweighted wake-sleep for models with stochastic control flow. *Association for Uncertainty in Artificial Intelligence*, 2019.
- [28] Eric Veach and Leonidas J Guibas. Optimally combining sampling techniques for monte carlo rendering. In *Proceedings of the 22nd annual conference on Computer graphics and interactive techniques*, 1995.
- [29] Michael E Tipping and Christopher M Bishop. Probabilistic principal component analysis. *Journal of the Royal Statistical Society: Series B (Statistical Methodology)*, 1999.
- [30] Pierre Simon Laplace. Memoir on the probability of the causes of events. *Statistical Science*, 1986.
- [31] Martin J. Wainwright. *High-Dimensional Statistics: A Non-Asymptotic Viewpoint*. Cambridge University Press, 2019.
- [32] Yann LeCun, Léon Bottou, Yoshua Bengio, Patrick Haffner, et al. Gradient-based learning applied to document recognition. *Proceedings of the IEEE*, 1998.
- [33] Diederik P Kingma and Jimmy Ba. Adam: A method for stochastic optimization. In *International Conference in Learning Representations*, 2015.
- [34] Diederik P Kingma, Shakir Mohamed, Danilo Jimenez Rezende, and Max Welling. Semi-supervised learning with deep generative models. In *Advances in Neural Information Processing Systems*, 2014.
- [35] Runjing Liu, Jeffrey Regier, Nilesh Tripuraneni, Michael Jordan, and Jon McAuliffe. Rao-Blackwellized stochastic gradients for discrete distributions. In *International Conference on Machine Learning*, 2019.
- [36] Allon Wagner, Aviv Regev, and Nir Yosef. Revealing the vectors of cellular identity with single-cell genomics. *Nature Biotechnology*, 2016.
- [37] Amos Tanay and Aviv Regev. Scaling single-cell genomics from phenomenology to mechanism. *Nature*, 2017.
- [38] Dominic Grun, Lennart Kester, and Alexander van Oudenaarden. Validation of noise models for single-cell transcriptomics. *Nature Methods*, 2014.
- [39] Michael B Cole, Davide Risso, Allon Wagner, David DeTomaso, John Ngai, Elizabeth Purdom, Sandrine Dudoit, and Nir Yosef. Performance assessment and selection of normalization procedures for single-cell RNA-seq. *Cell Systems*, 2017.
- [40] Michael I. Love, Wolfgang Huber, and Simon Anders. Moderated estimation of fold change and dispersion for RNA-seq data with DESeq2. *Genome Biology*, 2014.
- [41] Pierre Boyeau, Romain Lopez, Jeffrey Regier, Adam Gayoso, Michael I. Jordan, and Nir Yosef. Deep generative models for detecting differential expression in single cells. In *Machine Learning in Computational Biology*, 2019.
- [42] Shiqi Cui, Subharup Guha, Marco A. R. Ferreira, and Allison N. Tegge. hmmSeq: A hidden Markov model for detecting differentially expressed genes from RNA-seq data. *The Annals of Applied Statistics*, 2015.
- [43] Xiuwei Zhang, Chenling Xu, and Nir Yosef. Simulating multiple faceted variability in single cell RNA sequencing. *Nature communications*, 2019.
- [44] Melanie F Pradier, Michael C Hughes, and Finale Doshi-Velez. Challenges in computing and optimizing upper bounds of marginal likelihood based on chi-square divergences. In *Symposium on Advances in Approximate Bayesian Inference*, 2019.
- [45] Simon Lacoste-Julien, Ferenc Huszár, and Zoubin Ghahramani. Approximate inference for the loss-calibrated Bayesian. In *International Conference on Artificial Intelligence and Statistics*, 2011.
- [46] Tomasz Kuśmierczyk, Joseph Sakaya, and Arto Klami. Variational Bayesian decision-making for continuous utilities. In *Advances in Neural Information Processing Systems*, 2019.
- [47] Yingzhen Li and Richard E Turner. Rényi divergence variational inference. In *Advances in Neural Information Processing Systems*, 2016.
- [48] Dilin Wang, Hao Liu, and Qiang Liu. Variational inference with tail-adaptive f-divergence. In *Advances in Neural Information Processing Systems*, 2018.
- [49] Beatrice Laurent and Pascal Massart. Adaptive estimation of a quadratic functional by model selection. *The Annals of Statistics*, 2000.
- [50] Jacob Burbea. The convexity with respect to gaussian distributions of divergences of order α . *Utilitas Mathematica*, 1984.
- [51] Yunchen Pu, Zhe Gan, Ricardo Henao, Xin Yuan, Chunyuan Li, Andrew Stevens, and Lawrence Carin. Variational autoencoder for deep learning of images, labels and captions. In *Advances in Neural Information Processing Systems*, 2016.
- [52] Daniel Hsu, Sham Kakade, Tong Zhang, et al. A tail inequality for quadratic forms of sub-Gaussian random vectors. *Electronic Communications in Probability*, 2012.
- [53] Krzysztof Zajkowski. Bounds on tail probabilities for quadratic forms in dependent sub-Gaussian random variables. *arXiv*, 2018.
- [54] Chuan Guo, Geoff Pleiss, Yu Sun, and Kilian Q. Weinberger. On calibration of modern neural networks. In *International Conference on Machine Learning*, 2017.

Supplementary Information

In Appendix A, we prove the theoretical results presented in this manuscript. In Appendix B, we present the analytical derivations in the bivariate Gaussian setting. In Appendix C we present a general analysis of Gaussian VAEs. In Appendix D, we provide details on the simulation framework for the pPCA experiments. In Appendix E, we discuss why alternative divergences would be especially suitable for the M1+M2 model. In Appendix F, we derive gradients updates for the CUBO and the EUBO objective functions. In Appendix G, we present the generative model used in the single-cell transcriptomics experiment.

A Proofs

A.1 Proof of Proposition 1

Proposition 1. (Deviation for posterior expectation estimates) *Let \mathcal{F} be a set of test functions uniformly bounded by 1 on \mathcal{Z} . Let $f \in \mathcal{F}$ and $\eta \in \mathbb{R}_+^*$. With probability at least $1 - \eta$ in (z_1, \dots, z_n) , we have that*

$$\begin{aligned} |\hat{Q}_p^n(f, x) - \mathcal{Q}(f, x)| &\leq \sqrt{\frac{\ln 1/\eta}{2n}} + \sqrt{\Delta_{KL}(p_\theta \parallel q_\phi)} \\ |\hat{Q}_{IS}^n(f, x) - \mathcal{Q}(f, x)| &\leq \frac{2B \ln 1/\eta}{3n} + \sqrt{\frac{2\Delta_{\chi^2}(p_\theta \parallel q_\phi) \ln 1/\eta}{n}}, \end{aligned}$$

where $B = \sup_{z \in \mathcal{Z}} w(x, z)$.

Proof. For the plugin estimator

$$\hat{Q}_p^n(f, x) = \frac{1}{n} \sum_{i=1}^n f(z_i), \quad (21)$$

we invoke the Hoeffding inequality [31] and Pinsker's inequality:

$$\left| \frac{1}{n} \sum_{i=1}^n f(z_i) - \mathbb{E}_{p(z|x)} f(z) \right| \leq \left| \frac{1}{n} \sum_{i=1}^n f(z_i) - \mathbb{E}_{q(z|x)} f(z) \right| + \left| \mathbb{E}_{q(z|x)} f(z) - \mathbb{E}_{p(z|x)} f(z) \right| \quad (22)$$

$$\leq \sqrt{\frac{\ln 1/\eta}{2n}} + \sup_{g \in \mathcal{F}} |\mathbb{E}_{q(z|x)} g(z) - \mathbb{E}_{p(z|x)} g(z)| \quad (23)$$

$$\leq \sqrt{\frac{\ln 1/\eta}{2n}} + 2\Delta_{TV}(p(z|x) \parallel q(z|x)) \quad (24)$$

$$\leq \sqrt{\frac{\ln 1/\eta}{2n}} + \sqrt{\Delta_{KL}(p(z|x) \parallel q(z|x))}. \quad (25)$$

For the importance sampling estimator

$$\hat{Q}_{IS}^n(f, x) = \frac{1}{n} \sum_{i=1}^n w(x, z_i) f(z_i), \quad (26)$$

we instead use a Bernstein bound as described in Theorem 1 of [22]. \square

A.2 Proof of Lemma 1

Lemma 1. (Concentration of the log-likelihood ratio) *For an observation x , let Σ be the variance of the posterior distribution under the pPCA model, $p_\theta(z|x)$. Let*

$$A(x) = \Sigma^{1/2} [D(x)]^{-1} \Sigma^{1/2} - I. \quad (12)$$

For z following the posterior distribution, $\log w(x, z)$ is a sub-exponential random variable. Further, there exists a $t^(x)$ such that, under the posterior $p_\theta(z|x)$ and for all $t > t^*(x)$,*

$$\mathbb{P}(|\log w(x, z) - \Delta_{KL}(p_\theta \parallel q_\phi)| \geq t) \leq e^{-\frac{t}{8\|A(x)\|_2}}, \quad (13)$$

Proof. Here we first give the closed-form expression of the posterior and then we prove the concentration bounds on the log-likelihood ratio. Let $M = W^\top W + \sigma^2 I$. For notational convenience, we do not explicitly denote dependence on random variable x .

Step 1: Tractable posterior. Using the Gaussian conditioning formula [17], we have that

$$p_\theta(z | x) = \text{Normal}(M^{-1}W^\top(x - \mu), \sigma^2 M^{-1}). \quad (27)$$

Step 2: Concentration of the log-ratio. For this, since x is a fixed point, we note $a = M^{-1}W^\top(x - \mu)$ and $b = \nu(x)$. We can express the log density ratio as

$$w(z, x) = \log \frac{p_\theta(z | x)}{q_\phi(z | x)} \quad (28)$$

$$= -\frac{1}{2} \log \det(\sigma^2 M^{-1} D^{-1}) - \frac{1}{2\sigma^2} (z - a)^\top M (z - a) + \frac{1}{2} (z - b)^\top D^{-1} (z - b) \quad (29)$$

$$= C + z^\top \left[\frac{D^{-1}}{2} - \frac{M}{2\sigma^2} \right] z + \left[D^{-1} b - \frac{M a}{\sigma^2} \right]^\top z, \quad (30)$$

where C is a constant. To further characterize the tail behavior, let ϵ be an isotropic multivariate normal distribution and express the log-ratio as a function of ϵ instead of the posterior probability. We have that $z = M^{-1}W^\top(x - \mu) + \sigma M^{-1/2} \epsilon$. The log ratio can now be written as

$$\log w(z, x) = C' + \epsilon^\top \left[\frac{\sigma^2 M^{-1/2} D^{-1} M^{-1/2} - I}{2} \right] \epsilon + \left[\sigma M^{-1/2} D^{-1} b - \frac{M^{1/2} a}{\sigma} \right]^\top \epsilon. \quad (31)$$

Because ϵ is isotropic Gaussian, we can compute the deviation of this log-ratio and provide concentration bounds. Because ϵ is Gaussian and $\epsilon \mapsto \log w(z, x)$ is a quadratic function, we show the log-ratio under the posterior is a sub-exponential random variable.

The following Lemma makes this statement precise, and it has a similar implication as the classic result in [49].

Lemma 2. *Let $d \in \mathbb{N}^*$ and $\epsilon \sim \text{Normal}(0, I_d)$. For matrix $A \in \mathbb{R}^{d \times d}$ and vector $b \in \mathbb{R}^d$, random variable $v = \epsilon^\top A \epsilon + b^\top \epsilon$ is sub-exponential with parameters $(\sqrt{2 \|A\|_F^2 + \|b\|_2^2/4}, 4 \|A\|_2)$. In particular, we have the following concentration bounds,*

$$\mathbb{P}[|v| \geq t] \leq 2 \exp \left\{ -\frac{t^2}{8 \|A\|_F^2 + \|b\|_2^2 + 4 \|A\|_2 t} \right\} \quad \text{for all } t > 0. \quad (32)$$

$$\mathbb{P}[|v| \geq t] \leq \exp \left\{ -\frac{t}{8 \|A\|_2} \right\} \quad \text{for all } t > \frac{8 \|A\|_F^2 + \|b\|_2^2}{16 \|A\|_2}. \quad (33)$$

For $A = \frac{\sigma^2 M^{-1/2} D^{-1} M^{-1/2} - I}{2}$ and $b = \sigma M^{-1/2} D^{-1} b - \frac{M^{1/2} a}{\sigma}$, we can apply Lemma 2. We deduce a concentration bound on the log-ratio around its mean, which is the forward Kullback-Leibler divergence $L = \Delta_{\text{KL}}(p_\theta(z | x) \| q_\phi(z | x))$. More precisely, we have that

$$p_\theta(|\log w(z, x) - L| \geq t | x) \leq 2 \exp \left\{ -\frac{t^2}{8 \|A\|_F^2 + \|b\|_2^2 + 4 \|A\|_2 t} \right\} \quad \text{for all } t > 0. \quad (34)$$

□

as well as the deviation bound for large t , which ends the proof.

A.3 Proof of Lemma 2

Proof. Let $\lambda \in \mathbb{R}^+$. We have that $\mathbb{E}v = \text{Tr}(A)$. We wish to bound the moment generating function

$$\mathbb{E}[e^{\lambda(v - \text{Tr}(A))}] = e^{-\lambda \text{Tr}(A)} \mathbb{E}[e^{\lambda(\epsilon^\top A \epsilon + b^\top \epsilon)}]. \quad (35)$$

Sums of arbitrary correlated variables are hard to analyze. Here we rely on the property that Gaussian vectors are invariant by rotation: Let $A = Q\Lambda Q^\top$ be the eigenvalue decomposition for A and denote $\epsilon = Q\xi$ as well as $b = Q\beta$. Since Q is an orthogonal matrix, ξ also follows an isotropic normal distribution and

$$\mathbb{E}[e^{\lambda(v - \text{Tr}(A))}] = e^{-\lambda \text{Tr}(A)} \mathbb{E}[e^{\lambda(\xi^\top \Lambda \xi + \beta^\top \xi)}] \quad (36)$$

$$= e^{-\lambda \text{Tr}(A)} \mathbb{E}\left[\prod_{i=1}^d e^{\lambda \xi_i^2 \Lambda_i + \lambda \beta_i \xi_i}\right] \quad (37)$$

$$= e^{-\lambda \text{Tr}(A)} \prod_{i=1}^d \mathbb{E}\left[e^{\lambda \xi_i^2 \Lambda_i + \lambda \beta_i \xi_i}\right] \quad (38)$$

$$= \prod_{i=1}^d \mathbb{E}\left[e^{\lambda \xi_i^2 \Lambda_i + \lambda \beta_i \xi_i - \lambda \Lambda_i}\right]. \quad (39)$$

Because each component ξ_i follows a isotropic Gaussian distribution, we can compute the moment generating functions in closed form

$$\mathbb{E}\left[e^{\lambda \xi_i^2 \Lambda_i + \lambda \beta_i \xi_i - \lambda \Lambda_i}\right] = \frac{e^{-\lambda \Lambda_i}}{\sqrt{2\pi}} \int_{-\infty}^{+\infty} e^{\lambda \Lambda_i u^2 + \lambda \beta_i u} e^{-\frac{u^2}{2}} du \quad (40)$$

$$= \frac{e^{-\lambda \Lambda_i}}{\sqrt{2\pi}} \int_{-\infty}^{+\infty} e^{[\lambda \Lambda_i - \frac{1}{2}]u^2 + \lambda \beta_i u} du. \quad (41)$$

This integral is convergent if and only if $\lambda < 1/2\Lambda_i$. In that case, we have after a change of variable that

$$\mathbb{E}\left[e^{\lambda \xi_i^2 \Lambda_i + \lambda \beta_i \xi_i - \lambda \Lambda_i}\right] = \frac{e^{-\lambda \Lambda_i}}{\sqrt{\pi} \sqrt{1 - 2\lambda \Lambda_i}} \int_{-\infty}^{+\infty} e^{-s^2 + \frac{\sqrt{2}\lambda \beta_i s}{\sqrt{1 - 2\lambda \Lambda_i}}} ds \quad (42)$$

$$= \frac{e^{-\lambda \Lambda_i} e^{\frac{\lambda^2 \beta_i^2}{2(1 - 2\lambda \Lambda_i)}}}{\sqrt{1 - 2\lambda \Lambda_i}}. \quad (43)$$

Then, using the fact that for $a < 1/2$, we have $e^{-a} \leq e^{2a^2} \sqrt{1 - 2a}$, we can further simplify for $\lambda < \frac{1}{4\Lambda_i}$

$$\mathbb{E}\left[e^{\lambda \xi_i^2 \Lambda_i + \lambda \beta_i \xi_i - \lambda \Lambda_i}\right] \leq e^{2\lambda^2 \Lambda_i^2 + \frac{\lambda^2 \beta_i^2}{2(1 - 2\lambda \Lambda_i)}} \quad (44)$$

$$\leq e^{[2\Lambda_i^2 + \frac{\beta_i^2}{4}]\lambda^2}. \quad (45)$$

Putting back all the components of ξ , we have that for all $\lambda < \frac{1}{4\|\Lambda\|_2} = \frac{1}{4\|A\|_2}$

$$\mathbb{E}[e^{\lambda(v - \text{Tr}(A))}] \leq \exp\left\{\left[2\|\Lambda\|_F^2 + \frac{\|\beta\|_2^2}{4}\right]\lambda^2\right\} \quad (46)$$

$$\leq \exp\left\{\left[2\|A\|_F^2 + \frac{\|b\|_2^2}{4}\right]\lambda^2\right\}, \quad (47)$$

where the last inequality is in fact an equality because Q is an isometry. Therefore, according to Definition 2.2 in [31], v is sub-exponential with parameters $(\sqrt{2\|A\|_F^2 + \|b\|_2^2}/4, 4\|A\|_2)$. The concentration bound is derived as in the proof of Proposition 2.3 in [31]. \square

A.4 Proof of Theorem 1

Theorem 1. (Sufficient sample size) *For an observation x , suppose that the second moment of $f(z)$ under the posterior is bounded by κ . If the number of particles for importance sampling n satisfies $n = \exp\{\Delta_{\text{KL}}(p_\theta \| q_\phi) + t\}$ for some $t > t^*(x)$, then*

$$\mathbb{E}|\hat{\mathcal{Q}}_{\text{IS}}^n(f, x) - \mathcal{Q}(f, x)| \leq 3\sqrt{\kappa}e^{-t/4\gamma}, \quad (14)$$

with $\gamma = \max(1, 4\|A(x)\|_2)$

Proof. By Theorem 1.1 from [25], for $t > t^*(x)$,

$$\mathbb{E}|\hat{\mathcal{Q}}_{\text{IS}}^n(f, x) - \mathcal{Q}(f, x)| \leq \sqrt{\kappa} \left(e^{-t/4} + 2e^{-\frac{t}{16\|A(x)\|_2}} \right). \quad (48)$$

The bound in Theorem 1 follows. \square

B Analytical derivations in the bivariate Gaussian setting

For a fixed x , we adopt the condensed notation $p_\theta(z | x) = p$. According to the Gaussian conditioning formula, there exists μ and Λ such that

$$p \sim \text{Normal}(\mu, \Lambda^{-1}).$$

We consider variational approximations of the form

$$q \sim \text{Normal}(\nu, \text{diag}(\lambda)^{-1}).$$

We wish to characterize the solution q to the following optimization problems

$$q_{\text{RKL}} = \arg \min_q \Delta_{\text{KL}}(q \| p), \quad q_{\text{FKL}} = \arg \min_q \Delta_{\text{KL}}(p \| q), \quad q_\chi = \arg \min_q \Delta_{\chi^2}(p \| q). \quad (49)$$

We focus on the setting where the mean of the variational distribution is correct. This is true for variational Bayes or the general Renyi divergence, as underlined in [47]). We therefore further assume ν can be chosen equal to μ for simplicity.

In the bivariate setting, we have conveniently an analytically tractable inverse formula:

$$\Lambda = \begin{bmatrix} \Lambda_{11} & \Lambda_{12} \\ \Lambda_{21} & \Lambda_{22} \end{bmatrix}, \quad \Lambda^{-1} = \frac{1}{|\Lambda|} \begin{bmatrix} \Lambda_{22} & -\Lambda_{12} \\ -\Lambda_{21} & \Lambda_{11} \end{bmatrix}, \quad (50)$$

We also rely on the expression of the Kullback-Leibler divergence between two multivariate Gaussian distributions of \mathbb{R}^d

$$\Delta_{\text{KL}}(\text{Normal}(\mu, \Sigma_1) \| \text{Normal}(\mu, \Sigma_2)) = \frac{1}{2} \left[\log \frac{|\Sigma_2|}{|\Sigma_1|} - d + \text{Tr}(\Sigma_2^{-1} \Sigma_1) \right]. \quad (51)$$

Reverse KL Using the expression of the KL and the matrix inverse formula, we have that

$$\arg \min_q \Delta_{\text{KL}}(q \| p) = \arg \min_{\lambda_1, \lambda_2} \log \lambda_1 \lambda_2 + \frac{\Lambda_{11}}{\lambda_1} + \frac{\Lambda_{22}}{\lambda_2}. \quad (52)$$

The solution to this optimization problem is

$$\begin{cases} \lambda_1 &= \Lambda_{11} \\ \lambda_2 &= \Lambda_{22} \end{cases}. \quad (53)$$

Forward KL From similar calculations,

$$\arg \min_q \Delta_{\text{KL}}(p \| q) = \arg \min_{\lambda_1, \lambda_2} -\log \lambda_1 \lambda_2 + \frac{1}{|\Lambda|} [\lambda_1 \Lambda_{22} + \lambda_2 \Lambda_{11}]. \quad (54)$$

The solution to this optimization problem is

$$\begin{cases} \lambda_1 &= \Lambda_{11} - \frac{\Lambda_{12} \Lambda_{21}}{\Lambda_{22}} \\ \lambda_2 &= \Lambda_{22} - \frac{\Lambda_{12} \Lambda_{21}}{\Lambda_{11}} \end{cases}. \quad (55)$$

Chi-square divergence A closed-form expression of the Renyi divergence for exponential families (and in particular multivariate Gaussian) is derived in [50]. We could in principle follow the same approach. However, [51] derived a similar results, which is exactly the wanted quantity for $\alpha = -1$ in Appendix B of their manuscript. Therefore, we simply report this result

$$\begin{cases} \lambda_1 &= \Lambda_{11} \left[\frac{3}{2} - \frac{1}{2} \sqrt{1 + \frac{8\Lambda_{12}\Lambda_{21}}{\Lambda_{11}\Lambda_{22}}} \right] \\ \lambda_2 &= \Lambda_{22} \left[\frac{3}{2} - \frac{1}{2} \sqrt{1 + \frac{8\Lambda_{12}\Lambda_{21}}{\Lambda_{11}\Lambda_{22}}} \right] \end{cases}. \quad (56)$$

C Theory for Gaussian VAEs

In order to extend the analysis we did in the setting of probabilistic PCA, we need to (i) characterize the tail behavior of the posterior distribution and (ii) characterize the tail behavior of the log-likelihood ratio. Consider the following setting:

$$p_\theta(z) = \text{Normal}(0, I_d) \quad (57)$$

$$p_\theta(x | z) = \text{Normal}(\mu(z), \Sigma) \quad (58)$$

$$q_\phi(z | x) = \text{Normal}(\nu(x), D(x)), \quad (59)$$

where $\Sigma = \text{diag}(\sigma_1^2, \dots, \sigma_p^2)$, $\mu(z) = W_1 \text{ReLU}(W_2 z + b_2) + b_1$ and $D(x) = \text{diag}(\lambda(x))$. We note $\Lambda = \Sigma^{-1}$ and $\Theta(x) = D^{-1}(x)$. Although in this setting μ is a one-layer neural network, the analysis holds for multiple layers as long as we can bound the one-norm of $\mu(z)$ as a function of the one-norm of z .

C.1 sub-Gaussian posterior

Under this setting, we can show that for each point x , the posterior $p_\theta(z | x)$ is sub-Gaussian.

Proposition 2. *In the Gaussian VAE described above, for each point $x \in \mathcal{X}$, the posterior $p_\theta(z | x)$ is a sub-Gaussian random variable. Namely, given $\mu^*(x)$ the mean of the posterior, there exists an optimal constant $\eta^*(x)$ such that*

$$\forall x \in \mathcal{X}, \forall \alpha \in \mathbb{R}^d, \mathbb{E} \left[\exp \{ \alpha^\top (z - \mu^*(x)) \} \mid x \right] \leq \exp \{ \|\alpha\|_2 \eta^*(x)^2 / 2 \} \quad (60)$$

Proof. Let $\alpha \in \mathbb{R}^d$ and $x \in \mathcal{X}$.

$$\mathbb{E} \left[e^{\alpha^\top z} \mid x \right] = \frac{1}{p_\theta(x)} \int e^{\alpha^\top z} p_\theta(x | z) p_\theta(z) dz \quad (61)$$

$$= \frac{e^{-\frac{x^\top \Lambda x}{2}}}{p_\theta(x) (2\pi)^{\frac{d+p}{2}} \prod_{i=1}^p \sigma_i} \int e^{\alpha^\top z - \frac{z^\top z}{2} + x^\top \Lambda \mu(z) - \frac{\mu(z)^\top \Lambda \mu(z)}{2}} dz \quad (62)$$

We now focus on the exponent of the integral and introduce the variable $h = W_2 z + b_2$ as well as the notation $h_+ = \text{ReLU}(h)$.

$$f(x, z, \alpha) = \alpha^\top z - \frac{z^\top z}{2} + x^\top \Lambda \mu(z) - \frac{\mu(z)^\top \Lambda \mu(z)}{2} \quad (63)$$

$$= \alpha^\top z - \frac{z^\top z}{2} + x^\top \Lambda W_1 h_+ + x^\top \Lambda b_1 - \frac{h_+^\top W_1^\top \Lambda W_1 h_+}{2} - b_1^\top \Lambda W_1 h_+ - \frac{b_1^\top \Lambda b_1}{2} \quad (64)$$

$$= \alpha^\top z - \frac{z^\top z}{2} + (x - b_1)^\top \Lambda W_1 h_+ - \frac{h_+^\top W_1^\top \Lambda W_1 h_+}{2} + x^\top \Lambda b_1 - \frac{b_1^\top \Lambda b_1}{2}. \quad (65)$$

For $\beta = W_1^\top \Lambda (x - b_1)$ and a constant $C(x)$, we therefore have that

$$\mathbb{E} \left[e^{\alpha^\top z} \mid x \right] = C(x) \mathbb{E}_{z \sim \mathcal{N}(0, I)} \left[e^{\alpha^\top z + \beta^\top h_+ - (W_1 h_+)^\top M_2 W_1 h_+} \right]. \quad (66)$$

Using Hölder's inequality, we can bound the dot product

$$\beta^\top h_+ \leq \|\beta\|_\infty \|h_+\|_1 \quad (67)$$

$$\leq \|\beta\|_\infty \|W_2 z + b_2\|_1 \quad (68)$$

$$\leq \|\beta\|_\infty \|W_2\|_1 (\|z\|_1 + \|b_2\|). \quad (69)$$

Then, observing that Λ is a PSD matrix and we can bound the MGF by

$$\mathbb{E} \left[e^{\alpha^\top z} \mid x \right] \leq \tilde{C}(x) \prod_{i=1}^d \mathbb{E}_{z_i \sim \mathcal{N}(0, 1)} \left[e^{\alpha_i z_i + \|\beta\|_\infty \|W_2\|_1 |z_i|} \right] \quad (70)$$

$$\leq \tilde{C}(x) e^{\|\alpha\|_2^2 + \|\beta\|_\infty^2 \|W_2\|_1^2}. \quad (71)$$

Plugging this MGF bound into a Chernoff bound, we get that

$$\mathbb{P} \left(e^{\alpha^\top z} \geq t \mid x \right) \leq C(x, W_1, W_2) e^{-\frac{t^2}{2}}. \quad (72)$$

This is a sub-Gaussian type of bound, which concludes the proof. \square

The result above is not sharp. Indeed, the sub-Gaussian parameter is a function of the constant C and we used lots of rough comparisons. We therefore assume we have at our disposal the optimal sub-Gaussian constant $\eta^*(x)$ for the rest of our analysis.

C.2 Concentration of the log-likelihood ratios

We show now that the log-likelihood ratio is a subexponential random variable for z sampled from the posterior. This is important to guarantee the most efficient rate in the theorem of [25]. As the optimal sub-exponential constant is hard to characterize for the VAE, we focus on this analysis on exhibiting the global tail behavior. We presented tighter bounds in the pPCA setting.

Proposition 3. *Let x be a fixed point. Further, assume that $f(z)$ has second moment under the posterior bounded by V . There exists a constant $t^*(x)$ and a constant $\rho^*(x)$ such that if $n = \exp\{\Delta_{KL}(p_\theta \parallel q_\phi) + t\}$ for some $t > t^*(x)$, we have that*

$$\mathbb{E} \left| \hat{Q}_{IS}(f) - \mathcal{Q}_{p_\theta}(f, x) \right| \leq \sqrt{V} \left(e^{-t/4} + e^{-\frac{t}{2\rho^*(x)}} \right). \quad (73)$$

Proof. We can write the exact expression of the log-likelihood ratios in our setting. Fix a point x in \mathcal{X} .

$$\log \frac{p_\theta(z | x)}{q_\phi(z | x)} = \log \frac{p_\theta(x, z)}{q_\phi(z | x)p_\theta(x)} \quad (74)$$

$$= K(x) - \frac{1}{2} (x - \mu(z))^\top \Lambda (x - \mu(z)) - \frac{1}{2} z^\top z + \frac{1}{2} (\nu(x) - z)^\top \Theta(x) (\nu(x) - z) \quad (75)$$

$$= \hat{K}(x) - \frac{1}{2} \mu(z)^\top \Lambda \mu(z) + \frac{1}{2} z^\top [\Theta(x) - I] z + x^\top \Lambda \mu(z) - \nu(x)^\top \Theta(x) z. \quad (76)$$

By introducing the same notation as previously, $h_+ = \text{ReLU}(W_1 z + b_1)$, we get the simplified expression

$$\log \frac{p_\theta(z | x)}{q_\phi(z | x)} = \hat{K}(x) + \frac{1}{2} z^\top [\Theta(x) - I] z - \nu(x)^\top \Theta(x) z - \frac{1}{2} h_+^\top W_2^\top \Lambda W_2 h_+ + x^\top \Lambda W_2 h_+. \quad (77)$$

We wish to derive an upper tail bound on the deviation of the log-likelihood ratio from its mean L (the forward KL divergence). Because of that, it suffices to prove concentration on an upper bound of the log-likelihood ratio. Using the fact that Λ is PSD and Hölder's inequality, we have

$$\log \frac{p_\theta(z | x)}{q_\phi(z | x)} \leq \hat{K}(x) + \frac{1}{2} z^\top [\Theta(x) - I] z - \nu(x)^\top \Theta(x) z + \|W_2^\top \Lambda x\|_\infty \|W_1\|_1 \|z\|_1. \quad (78)$$

This bound will be enough to prove a sub-exponential concentration bound, although is much too crude to extract optimal constants (which we get up to universal constants in the pPCA setting). Still, we are reducing the problem to analyzing a near-quadratic function of sub-Gaussian random variables. We can therefore adapt results for quadratic forms of sub-Gaussian random variables, as the one in [52].

For convenience, we consider now the following functional

$$f : z \mapsto \frac{1}{2} z^\top M z + \beta^\top z + \gamma \|z\|_1, \quad (79)$$

for which we wish to show that the random variable $f(z)$ is sub-exponential. We recall that z is a sub-Gaussian random variable and satisfies Equation (2). The main idea of this proof is to separate the different terms using a singular value decomposition and applying multiple times Hölder's inequality to provide a bound of the MGF. Let $\lambda \in \mathbb{R}$. For $x \in \mathcal{X}$, we have that (we drop the conditional expectation for convenience of notations):

$$\mathbb{E} \left[e^{\lambda f(z)} \right] = \mathbb{E} \left[e^{\frac{\lambda}{2} z^\top M z + \lambda \beta^\top z + \lambda \gamma \|z\|_1} \right] \quad (80)$$

$$\leq \underbrace{\left(\mathbb{E} \left[e^{\frac{3}{2} \lambda z^\top M z} \right] \right)^{\frac{1}{3}}}_{(i)} \underbrace{\left(\mathbb{E} \left[e^{3 \lambda \beta^\top z} \right] \right)^{\frac{1}{3}}}_{(ii)} \underbrace{\left(\mathbb{E} \left[e^{3 \lambda \gamma \|z\|_1} \right] \right)^{\frac{1}{3}}}_{(iii)}. \quad (81)$$

We can now analyze each term independently and prove that each one of them satisfies a sub-exponential bound.

(i) The first term can be bounded applying Hölder's inequality. Let $M = USU^\top$, with U orthogonal and S diagonal. Let e_i denote the i -th vector of the canonical basis of \mathbb{R}^d . Note that $\sum_{i=1}^d s_i = \|M\|_F$. Using the proof technique from [53], we have that

$$\mathbb{E} \left[e^{\frac{3}{2} \lambda z^\top M z} \right] = \mathbb{E} \left[e^{\frac{3}{2} \lambda \sum_{i=1}^d s_i (z^\top U e_i)^2} \right] \quad (82)$$

$$= \mathbb{E} \left[\prod_{i=1}^d e^{\frac{3}{2} \lambda s_i (z^\top U e_i)^2} \right] \quad (83)$$

$$\leq \prod_{i=1}^d \left(\mathbb{E} \left[e^{\frac{3}{2} \lambda \|M\|_F (z^\top U e_i)^2} \right] \right)^{\frac{s_i}{\|M\|_F}}. \quad (84)$$

Then, it suffices to bound all the individual integrals. Using the Cauchy-Schwartz inequality, we have that $(z^\top U e_i)^2 \leq \|z\|_2$. Since z is sub-Gaussian of parameter $\eta^*(x)$, $\|z\|_2$ is sub-exponential of parameter $\eta^*(x)^2$. That is, there exists a constant C_1 such that for all $\lambda < \frac{C_1}{\|M\|_F^2 \eta^*(x)^2}$,

$$\mathbb{E} \left[e^{\frac{3}{2} \lambda z^\top M z} \right] \leq e^{\frac{9}{4} \lambda^2 \|M\|_F^2 \eta^*(x)^4} \quad (85)$$

and it is known that this MGF would not have an upper bound for larger values of λ .

(ii) The second term is simply the standard bound of the MGF of a sub-Gaussian random vector. For all λ in \mathbb{R} , we have

$$\mathbb{E} \left[e^{3\lambda \beta^\top z} \right] \leq e^{9\lambda^2 \|\beta\|_2^2 \eta^*(x)^2}. \quad (86)$$

(iii) The last term is slightly irregular, and comes from the bound on the linear rectifier. Interestingly, the norm of a sub-Gaussian vector does concentrate but with a rate that usually depends on the dimension. This is also the case here, as for example the mean of the one-norm of the vector z is not anymore zero. Still, we can tensorise and bound the MGF

$$\mathbb{E} \left[e^{3\lambda \gamma \|z\|_1} \right] = \mathbb{E} \left[e^{3\lambda \gamma \sum_{i=1}^d |z_i|} \right] \quad (87)$$

$$= \mathbb{E} \left[\prod_{i=1}^d e^{3\lambda \gamma |z_i|} \right] \quad (88)$$

$$\leq \prod_{i=1}^d \left(\mathbb{E} \left[e^{3d\lambda \gamma |z_i|} \right] \right)^{\frac{1}{d}}. \quad (89)$$

Then, for a centered univariate σ^2 -sub-Gaussian random variable u ,

$$\mathbb{E} \left[e^{\lambda |u|} \right] = \int_{u>0} e^{\lambda u} du + \int_{u<0} e^{-\lambda u} du \leq 2e^{\frac{\lambda^2 \sigma^2}{2}}. \quad (90)$$

This inequality lets us express our bound as

$$\mathbb{E} \left[e^{3\lambda \gamma \|z\|_1} \right] \leq 2^{\frac{1}{d}} e^{9\lambda^2 \gamma^2 d \eta^*(x)^2}. \quad (91)$$

□

D Linear Gaussian Systems experiments

Let $(n, k, d) \in \mathbb{N}^3$, $A = [a_1, \dots, a_n]$, $C = [c_1, \dots, c_k]$, $\lambda \in \mathbb{R}^+$. We choose our linear system with random matrices:

$$\begin{aligned} \forall j \leq n, a_j &\sim \text{Normal} \left(0, \frac{I_d}{n} \right) \\ \forall j \leq k, c_j &\sim \text{Normal} \left(0, \frac{I_d}{k} \right). \end{aligned} \quad (92)$$

We define the conditional covariance

$$\Sigma_{x|z} = \lambda I_d + C C^\top. \quad (93)$$

Having drawn these parameters, the generative model is:

$$\begin{aligned} z &\sim \text{Normal} (0, I_n) \\ x | z &\sim \text{Normal} (A z, \Sigma_{x|z}). \end{aligned} \quad (94)$$

The marginal log-likelihood $p(x)$ is tractable:

$$x \sim \text{Normal} (0, \Sigma_{x|z} + A A^\top). \quad (95)$$

The posterior $p(z | x)$ is also tractable:

$$\begin{aligned} \Sigma_{z|x}^{-1} &= I_n + A^\top \Sigma_{x|z}^{-1} A \\ M_{z|x} &= \Sigma_{z|x} A^\top \Sigma_{x|z}^{-1} \\ z | x &\sim \text{Normal} (M_{z|x} x, \Sigma_{z|x}). \end{aligned} \quad (96)$$

The posterior expectation for a toy hypothesis testing $p(z_1 \geq \nu | x)$ (with $f : z \mapsto \mathbb{1}_{\{z_1 \geq \nu\}}$) is tractable too because this distribution is Gaussian and has a tractable cumulative distribution function.

E Analysis of alternate divergences for the M1+M2 model

We have the following pathological behavior, similar to the one presented in the factor analysis instance. This ill-behavior is further exacerbated when the M1+M2 model is fitted with a composite loss as in Equation 9 of [34]. Indeed, neural networks are known to have poorly calibrated uncertainties [54].

Proposition 4. *Consider the model defined in Eq. (15). Assume that posterior inference is exact for latent variables u and z , such that $q_\phi(z|x)q_\phi(u|c,z) = p_\theta(z,u|c,x)$. Further, assume that for a fixed $z \in \mathcal{Z}$, $p_\theta(c|z)$ has complete support. Then, as $\mathbb{E}_{q_\phi(c|z)} \log q_\phi(c|z) \rightarrow 0$, it follows that*

1. $\Delta_{\text{KL}}(q_\phi(c, z, u | x) \| p_\theta(c, z, u | x))$ is bounded;
2. $\Delta_{\text{KL}}(p_\theta(c, z, u | x) \| q_\phi(c, z, u | x))$ diverges; and
3. $\Delta_{\chi^2}(p_\theta(c, z, u | x) \| q_\phi(c, z, u | x))$ diverges.

Proof. The proof mainly consists in decomposing the divergences. The posterior for unlabelled samples factorizes as

$$p_\theta(c, u, z | x) = p_\theta(c | z)p_\theta(z, u | x, c). \quad (97)$$

From this, expression of the other divergences follow under the semi-exact inference hypothesis. Remarkably, all three divergences can be decomposed in similar forms. Also, the expression of the divergences can be written in closed form (recall that c is discrete) and as a function of λ .

Reverse-KL. In this case, the Kullback-Leibler divergence can be written as

$$\begin{aligned} \Delta_{\text{KL}}(q_\phi(c, z, u | x) \| p_\theta(c, z, u | x)) &= \mathbb{E}_{q_\phi(c|z)} \Delta_{\text{KL}}(q_\phi(z, u | x, c) \| p_\theta(z, u | x, c)) \\ &\quad + \mathbb{E}_{q_\phi(z|x)} \Delta_{\text{KL}}(q_\phi(c | z) \| p_\theta(c | z)), \end{aligned} \quad (98)$$

which further simplifies to

$$\Delta_{\text{KL}}(q_\phi(c, z, u | x) \| p_\theta(c, z, u | x)) = \mathbb{E}_{p_\theta(z|x)} \Delta_{\text{KL}}(q_\phi(c | z) \| p_\theta(c | z)).$$

This last equation can be rewritten as a constant plus the differential entropy of $q_\phi(c|z)$, which is bounded by $\log C$ in absolute value.

Forward-KL. Similarly, we have that

$$\begin{aligned} \Delta_{\text{KL}}(p_\theta(c, z, u | x) \| q_\phi(c, z, u | x)) &= \mathbb{E}_{p_\theta(c|z)} \Delta_{\text{KL}}(p_\theta(z, u | x, c) \| q_\phi(z, u | x, c)) \\ &\quad + \mathbb{E}_{p_\theta(z|x)} \Delta_{\text{KL}}(p_\theta(c | z) \| q_\phi(c | z)), \end{aligned}$$

which also further simplifies to

$$\begin{aligned} \Delta_{\text{KL}}(p_\theta(c, z, u | x) \| q_\phi(c, z, u | x)) &= \mathbb{E}_{p_\theta(z|x)} \Delta_{\text{KL}}(p_\theta(c | z) \| q_\phi(c | z)) \\ &= \mathbb{E}_{p_\theta(z|x)} \sum_{c=1}^C p_\theta(c | z) \log \frac{p_\theta(c | z)}{q_\phi(c | z)}. \end{aligned}$$

This last equation includes terms in $p_\theta(c|z) \log q_\phi(c|z)$, which are unbounded whenever $q_\phi(c|z)$ is zero but $p_\theta(c|z)$ is not.

Chi-square. Finally, for this divergence, we have the decomposition

$$\Delta_{\chi^2}(p_\theta(c, z, u | x) \| q_\phi(c, z, u | x)) = \mathbb{E}_{q_\phi(z,c,u|x)} \frac{p_\theta^2(z, u | x, c) p_\theta^2(c | z)}{q_\phi^2(z, u | x, c) q_\phi^2(c | z)},$$

which in that case simplifies to

$$\Delta_{\chi^2}(p_\theta(c, z, u | x) \| q_\phi(c, z, u | x)) = \mathbb{E}_{p_\theta(z|x)} \Delta_{\chi^2}(p_\theta(c | z) \| q_\phi(c | z)).$$

Similarly, the last equation includes terms in $p_\theta^2(c|z)/q_\phi(c|z)$, which are unbounded whenever $q_\phi(c|z)$ is zero but $p_\theta(c|z)$ is not. \square

F Extension of sbVAEs to the M1+M2 model

Here we derive the optimizer updates for fitting the M1+M2 model within the sbVAE framework. For labelled observations, the updates are similar to the updates for the standard VAE. We therefore focus on deriving gradients estimators for unlabelled observations. The gradient for the generative model is also identical to the ones in the original M1+M2 publication [34], so we focus on the gradients for the upper bounds.

F1 Chi-square divergence

Recall that the CUBO loss can be expressed as

$$\begin{aligned} CUBO^2 &:= \frac{1}{2} \mathbb{E}_{q_\phi(z, u, c | x)} \left[\left(\frac{p_\theta(x, z, u, c)}{q_\phi(z, u, c | x)} \right)^2 \right] \\ &= \frac{1}{2} \sum_{c=1}^C \mathbb{E}_{q_\phi(z|x)q_\phi(u|c,z)} \left[q_\phi(c | z) \left(\frac{p_\theta(x, z, u, c)}{q_\phi(z, u, c | x)} \right)^2 \right]. \end{aligned}$$

We use the reparameterization trick so that $z = g_z(x, \epsilon_z)$ and $u = g_u(z, c, \epsilon_u)$, where ϵ_z and ϵ_u are external noise variables. to derive that

$$\begin{aligned} \nabla_\phi CUBO^2 &= \frac{1}{2} \sum_{c=1}^C \mathbb{E}_{\epsilon_u, \epsilon_z} \left[\nabla_\phi \left[q_\phi(c | z) \left(\frac{p_\theta(x, z, u, c)}{q_\phi(z, u, c | x)} \right)^2 \right] \right] \\ &= \frac{1}{2} \sum_{c=1}^C \mathbb{E}_{\epsilon_u, \epsilon_z} \left[\nabla_\phi \left(\frac{p_\theta(x, z, u, c)}{q_\phi(z | x) \sqrt{q_\phi(c | z)} q_\phi(u | z, c)} \right)^2 \right] \\ &= \frac{1}{2} \sum_{c=1}^C \mathbb{E}_{\epsilon_u, \epsilon_z} \left[\nabla_\phi \left(\frac{p_\theta(x, z, u, c)}{q_\phi(z | x) \sqrt{q_\phi(c | z)} q_\phi(u | z, c)} \right)^2 \right]. \end{aligned}$$

For $w(x, z, u, c) := \frac{p_\theta(x, z, u, c)}{q_\phi(z|x)\sqrt{q_\phi(c|z)}q_\phi(u|z,c)}$,

$$\nabla_\phi CUBO^2 = \sum_{c=1}^C \mathbb{E}_{\epsilon_u, \epsilon_z} \left[w(x, z, u, c)^2 \nabla_\phi \log w(x, z, u, c) \right].$$

Let $d\{(z_k, u_k), 1 \leq k \leq K\}$ denote K particles. We approximate this gradient with

$$\nabla_\phi CUBO^2 \approx \frac{1}{K} \sum_{c=1}^C \sum_{k=1}^K w(x, z_k, u_k, c)^2 \nabla_\phi \log w(x, z_k, u_k, c).$$

F2 Forward KL divergence

We now derive a stable gradient estimator for the forward KL

$$\Delta_{\text{KL}}(p_\theta(z, c, u | x) \| q_\phi(z, c, u | x)) = \mathbb{E}_{p_\theta(z, u, c | x)} \log \frac{p_\theta(z, c, u | x)}{q_\phi(z, c, u | x)}.$$

This gradient of this loss with respect to ϕ becomes:

$$\begin{aligned} \mathbb{E}_{p_\theta(z, u, c | x)} \nabla_\phi \log \frac{p_\theta(z, c, u | x)}{q_\phi(z, c, u | x)} &= \mathbb{E}_{p_\theta(z, u, c | x)} \nabla_\phi \log \frac{p_\theta(z, c, u, x)}{q_\phi(z, c, u | x)} \\ &= \mathbb{E}_{p_\theta(c)} \mathbb{E}_{p_\theta(z, u | x, c)} \nabla_\phi \log \frac{p_\theta(z, c, u, x)}{q_\phi(z, c, u | x)} \\ &= \sum_{c=1}^C p_\theta(c) \times \mathbb{E}_{p_\theta(z, u | x, c)} \nabla_\phi \log \frac{p_\theta(z, c, u, x)}{q_\phi(z, c, u | x)}. \end{aligned}$$

As $p_\theta(z, u | x, c)$ is intractable, we employ self-normalized importance sampling using candidate distribution

$$Q_y(z, u) := q_\phi(z | x) q_\phi(u | z, c = y).$$

so that the gradient can be expressed as

$$\sum_{c=1}^C p_\theta(c) \times \mathbb{E}_{Q_c(z, u)} \left[\frac{p_\theta(z, u | x, c)}{Q_c(z, u)} \nabla_\phi \log \frac{p_\theta(z, c, u, x)}{q_\phi(z, c, u | x)} \right].$$

This is in turn approximated with importance sampling as

$$\sum_{c=1}^C p_\theta(c) \sum_{k=1}^K \hat{w}_k^c \nabla_\phi \log \frac{p_\theta(z_k, c, u_k, x)}{q_\phi(z_k, c, u_k | x)},$$

where z_k, u_k are identically independently distributed samples from associated variational posteriors and where

$$\hat{w}_k^c = \frac{\frac{p_\theta(z_k, u_k, x, c)}{q_\phi(z_k | x) q_\phi(u_k | z_k, c)}}{\sum_j \frac{p_\theta(z_j, u_j, x)}{q_\phi(z_j | x) q_\phi(u_j | z_j, c)}}.$$

G Generative model for single-cell RNA-seq data

We introduce here a variant of scVI as a generative model of cellular expression counts. For more information about scVI, please refer to the original publication [7].

Brief background on scVI Latent variable $z_n \sim \text{Normal}(0, I_d)$ represents the biological state of cell n . Latent variable $l_n \sim \text{LogNormal}(\mu_l, \sigma_l^2)$ represents the library size (a technical factor account for sampling noise in scRNA-seq experiments). Let f_w be a neural network. For each gene g , expression count x_{ng} follows a zero-inflated negative binomial distribution, whose negative binomial mean is the product of the library size l_n and normalized mean $h_{ng} = f_w(z_n)$. The normalized mean h_{ng} is therefore deterministic conditional on z_n ; it will have the uncertainty in the posterior due to z_n . The measure $p_\theta(h_{ng} | x_n)$ denotes the push-forward of $p_\theta(z_n | x_n)$ through the g -th output neuron of neural net f_w . scVI therefore models the distribution $p_\theta(x)$.

Differences introduced In our experiments, the importance sampling weights for all inference mechanisms had high values of PSIS diagnostic for the original scVI model. Although the FDR control was more efficient with alternative divergences, our proposal distributions were poor. The posterior variance for latent variable l_n could reach high values, leading to numerical instabilities for the importance sampling weights (at least on this dataset). To work around the problem, we removed the prior on l_n and learned a generative model for the conditional distribution $p_\theta(x_n | l_n)$ using the number of transcripts in cell n as a point estimate of l_n .